Mutational Analysis of the Interaction between Active Site Residues and the Loop Region in Mammalian Purple Acid Phosphatases†

Enrico G. Funhoff,‡ Jenny Ljusberg,§ Yunling Wang,§ Goran Andersson,§ and Bruce A. Averill*,‡,||

Swammerdam Institute for Life Sciences, University of Amsterdam, Plantage Muidergracht 12, 1018 TV Amsterdam, The Netherlands, and Karolinska Institutet, Huddinge University Hospital, Division of Pathology F 64, S-14186, Huddinge, Sweden

Received April 16, 2001; Revised Manuscript Received July 25, 2001

ABSTRACT: Mammalian purple acid phosphatases (PAPs) can be divided into two groups, which exhibit distinct spectroscopic and kinetics properties: PAPs that consist of a single 36 kDa polypeptide, and PAPs that have undergone limited proteolysis to give two fragments with masses of 16 and 20 kDa, respectively. Proteolysis results in an increase in enzymatic activity, an increase in the optimal pH for activity, and a change in the g_z value of the characteristic EPR spectrum of the mixed-valence binuclear iron center. It has been proposed that these changes are due to the loss of interactions between Asp146 in an exposed loop region and active site residues upon proteolysis. In the present study, site-directed mutagenesis of Asp146 in recombinant rat bone PAP (recRPAP) has confirmed this hypothesis. Conversion of Asp146 into Ala, which eliminates the interaction of the side chain with the active site, resulted in an enzyme with properties typical of PAPs isolated in proteolytically cleaved forms. The Asp146Asn and Asp146Glu mutants were also prepared and examined to assess the effects of altered electrostatic interactions and side-chain length. Limited proteolysis of all three mutant enzymes with cathepsin L resulted in a significant increase in catalytic activity. Thus, although the interaction between Asp146 and (an) active site residue(s) is the major factor responsible for the low catalytic activity of uncleaved PAPs, other interactions are also important. Since both *p*-nitrophenyl phosphate and osteopontin, a potential in vivo substrate, show the same level of activation, the observed increase in catalytic activity upon proteolysis is likely to be due to electrostatic rather than steric effects. EPR spectra of FeZn-recRPAP before and after cleavage by cathepsin L suggest that cleavage primarily affects the divalent metal site. The observation that p$K_{es,1}$ is also sensitive to changes at the divalent site is consistent with the proposal that the nucleophilic hydroxide is that bridging the divalent and trivalent metals.

The iron-containing purple acid phosphatases (PAPs)[1] are found in mammalian, plant, fungal, and bacterial sources (*1*, *2*). Mammalian PAPs contain an FeFe active site and typically are monomeric proteins with a molecular mass of 36 kDa. In contrast, plant PAPs contain either an FeZn or an FeMn metal center and are typically dimers of 55 kDa subunits (*2*, *3*). Although the similarities in their primary sequences are modest, the active site structure and the residues coordinating the active site are identical in mammalian and plant PAPs. A recent search of the genomic databases, however, identified new PAP sequences in plants that are not homologues of the known plant PAPs, but which have a predicted molecular mass of 35−40 kDa, and appear to be more closely related to the mammalian PAPs (*4*).

In most cases, the specific physiological function of PAPs is not yet clear (*5*). In pigs, PAP apparently functions in the transport of Fe to transferrin (*6*, *7*). In general, PAPs exhibit a broad hydrolytic activity toward phosphate esters in vitro (*8*, *9*), pointing to a degradative function in PAP-expressing cells such as bone marrow cells and macrophages. Studies on PAP "knockout" mice show that the enzyme is essential for normal bone resorption and mineralization in developing bones (*10*). Overexpression of PAP in mice results in incresed resorption of trabecular bone and mild osteoporosis (*11*). The recent demonstration that PAP is also present in dendritic cells suggests that PAP may function in regulating intracellular signaling pathways that control trafficking of MHC Class II-containing vesicles involved in antigen presentation (*12*). Osteopontin, a phosphoprotein that has been proposed to be the in vivo substrate of PAP, is apparently involved in both bone degradation and the immune system (*13*, *14*), consistent with a relationship between PAP activity and the immune response.

† This research was supported by a grant from the EU Biotechnology Program (Contract B104-CT-98-0385).

* To whom correspondence should be addressed. Phone: ++1-419-530-1585; Fax: ++1-419-530-1586; E-mail: baa@utoledo.edu.

‡ University of Amsterdam.

§ Huddinge University Hospital.

|| Current address: Department of Chemistry, University of Toledo, 2801 W. Bancroft Rd., Toledo, OH 43606-3390.

[1] Abbreviations: PAP, purple acid phosphatase; recRPAP, recombinant purple acid phosphatase from rat bone; Uf, purple acid phosphatase from pig uterine fluids; recHPAP, recombinant purple acid phosphatase from human placenta; PP, protein phosphatase; *p*-NPP, *p*-nitrophenyl phosphate; MOI, multiplicity of infection; IPTG, isopropylthio-*β*-D-galactoside; MES, 2-(*N*-morpholino)ethanesulfonic acid; HEPES, *N*-(2-hydroxyethyl)piperazine-*N*′-2-ethanesulfonic acid; TRIS, tris(hydroxymethyl)aminomethane; DTT, dithiothreitol; PVDF, polyvinylidene difluoride; EDTA, ethylenediaminetetraacetate; NBT/BCIP, nitro blue tetrazolium chloride/5-bromo-4-chloroindol-3-yl phosphate *p*-toluidine salt.

10.1021/bi010766r CCC: $20.00
Published on Web 08/29/2001

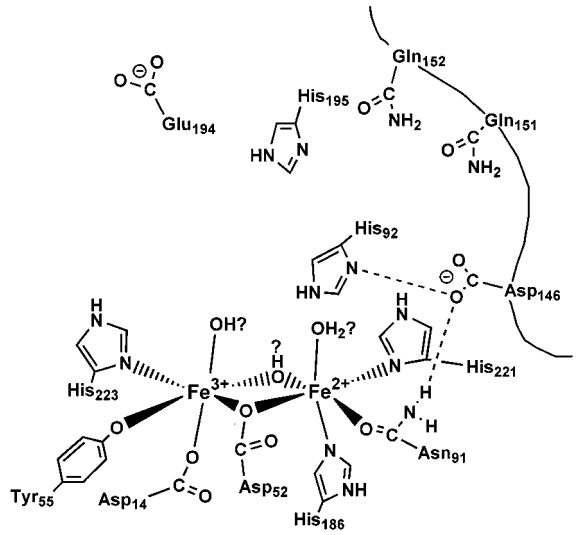

FIGURE 1: Schematic representation of the active site of PAP with numbering according to the human sequence.

The X-ray structure of kidney bean PAP showed that the active site contained a zinc ion coordinated by two histidines and an asparagine, and a ferric ion coordinated by a tyrosine, a histidine, and an aspartate residue (*15*). The two metal ions are bridged by a hydroxide and an aspartate carboxylate (schematic representation, Figure 1). Crystal structures of three mammalian PAPs [uteroferrin, Uf, at 1.5 Å resolution (*16*) and recombinant rat bone PAP, recRPAP, at 2.2 Å (*17*) and 2.7 Å resolution (*18*)] have recently been reported. All three proteins have highly symmetrical structures consisting of four α-helices coupled by *β*-sheets. The active site is found at the top of the protein in the vicinity of two exposed loops [residues 18−24 and 145−160; numbering according to the human sequence (*38*)]. The latter is absent in the 2.7 Å resolution rat bone structure, although the residues coordinating the metal center are completely conserved in all mammalian PAPs. One of the residues proposed to interact with substrate differs in plant and mammalian PAPs: His295 in the former is replaced by Glu194 in the latter (*15, 19*). The residues coordinated to the binuclear active site of the regulatory Ser/Thr protein phosphatases (PPs) are essentially identical to those in PAPs (*20*−*23*), as previously proposed based on the presence of a phosphoesterase motif (*24*). PPs, however, lack the tyrosinate coordinated to the Fe^{3+} metal ion that is responsible for the purple color, and instead contain a solvent molecule coordinated to the Fe^{3+}. The amino acids that interact with substrate in the PPs are one histidine (His92, according to the human sequence), which is conserved in all PAPs and PPs, and two arginines. Based on the high degree of similarity between the active sites of PAPs and PPs, it seems likely that both enzymes utilize similar mechanisms [for an extensive review on PP2B, see Rusnak et al. (*25*)].

Mammalian PAPs are known to be activated by proteolytic cleavage. For example, BSPAP is activated 4-fold at pH 6.0 by trypsin cleavage (*26*), while an 8-fold increase in activity at pH 5.8 is found for recRPAP (*9*) treated with cysteine proteases such as cathepsin B. Trypsin cleavage of recombinant human PAP (recHPAP) results in a 4-fold activation, when the activities at the optimal pH for both the intact and cleaved forms are compared (*27*). Activation is accompanied by a shift in pH optimum, from 4.8 to 5.9 for recRPAP and from 5.5 to 6.3 for recHPAP (*9, 27*). Proteolytic cleavage also converts the EPR spectrum from one that is characteristic of single-polypeptide PAPs (with features at $g_{xyz} = 1.58$, 1.73, and 1.94) into one characteristic of proteolytically cleaved PAPs (with features at $g_{xyz} = 1.60$, 1.73, and 1.86 at pH 5.0 as observed for recHPAP). In addition, mass spectrometric studies on recHPAP (*27*) and SDS−PAGE studies of recRPAP (*9*) showed that proteolytic cleavage excises a portion of a highly exposed loop near the active site. It has been proposed that the differences in both kinetics and spectroscopic characteristics reported for mammalian PAPs are due to changes in interactions between the loop and the active site upon cleavage (*27*).

Careful examination of the structures of Uf and recRPAP suggested that two interactions between the loop and the active site could be responsible for the observed differences between intact and proteolytically cleaved PAPs: that between Asp146 and either Asn91 or His92, both of which are conserved active site residues in all PAPs and PPs (*27*). Proteolytic cleavage would result in the loss of interaction between Asp146 and Asn91, destabilizing an Asn91 resonance structure which contains a C−N double bond and a polarized carboxylate oxygen, which is a better metal ligand. Thus, upon proteolysis, the Lewis acidity of the divalent metal ion would increase with a concomitant increase in the electrophilicity of the enzyme-bound substrate (assuming that the substrate coordinates to the divalent metal ion).

In the present study, we prepared mutants of Asp146 to explore the molecular basis for the relationship between proteolytic cleavage and enzymatic activation. Kinetics and spectroscopic characterization of the mutants demonstrated that interactions between Asp146 and the active site are primarily responsible for the differences observed between the single polypeptide and proteolytically cleaved forms of PAPs. Limited proteolysis of the mutant enzymes showed that further activation was possible, suggesting the presence of additional interactions between the loop residues and the active site that affect catalytic activity. Finally, the properties of the FeZn form of wild-type recRPAP, before and after cathepsin L cleavage, suggest that the interaction between Asp146 and Asn91, which primarily affects the divalent metal site, is likely to be more important than that between Asp146 and His92, which primarily affects the trivalent metal site.

EXPERIMENTAL PROCEDURES

Materials. Restriction enzymes, the DNA purification system, Cellfect, and the baculovirus expression system were purchased from Life Technologies. Excell 405 SFM was obtained from JRH Bioscience, *p*-nitrophenyl phosphate (*p*-NPP) from Fluka, and cathepsin L (219402) from Calbiochem (CH). All other chemicals were of the highest purity commercially available.

General Procedures. Enzyme concentrations were determined by measuring the absorbance of the Tyr^{-}- to-Fe^{3+} charge transfer at λ_{max} (510−550 nm, depending on the form; $\epsilon = 4080\ M^{-1}\ cm^{-1}$) on a Cary 50 spectrophotometer.

Recombinant baculovirus stocks containing coding regions for recRPAP or the D146A, D146E, and D146N mutants were used to infect High 5 cells cultured in 500−1000 mL of Excel 405 SFM at 27 °C; the cell density was 0.8×10^6

cells/mL, and a low MOI (0.001−0.01) was used. After 6 days, the cells were removed by centrifugation (10000*g*), and the enzyme was purified from the medium.

For the preparation of FeZn-recRPAP, metal-free buffer was prepared by passing it through a Chelex-100 column. A Sephadex G-25 column was eluted with a solution containing 5 mM ascorbic acid and 1 mM *o*-phenanthroline to remove excess metals, and subsequently eluted with metal-free Millipore water and a metal-free solution containing 40 mM NaOAc buffer, 1.6 M KCl, and 20% glycerol in Millipore water.

Generation of RecRPAP Mutants. Rat PAP cDNA [1.4 kb (*29*)] was cloned into a pCMV5 vector, and site-directed mutagenesis was performed using the 5′→3′ MORPH site-specific plasmid DNA mutagenesis kit (5 Prime → 3 Prime Inc., Boulder, CO). Primers used for each specific mutation were as follows: D146E, 5′-GCAATTCCGAAGACTTTGT-CAG-3; D146A, 5′-GTGGCAATTCCGCCGACTTTGT-CAG-3′; D146N, 5′-GCAATTCCAACGACTTTGTCAG-3′. The underlined bases indicate changes compared to the wild-type sequence. The primers employed for mutagenesis were phosphorylated by T4 kinase according to the manufacturer's instructions. DNA sequencing of the recRPAP mutants was used to verify the sequence (Cybergene AB, NOVUM, Huddinge, Sweden). Wild-type or mutant RPAP cDNAs were cloned into the baculovirus expression vector pFAST-BAC1 donor plasmid using the *Eco*RI restriction site. The proper orientation was determined by *Pst*I cleavage, and confirmed by DNA sequencing. The pFASTBAC1 donor vectors containing wild-type or mutant RPAP cDNAs were transformed into DH10Bac cells for homologous recombination with bacmid. Recombinant bacmids were selected by Luria agar plates containing antibiotics and IPTG (50 μg/mL kanamycin, 7 μg/mL gentamycin, 10 μg/mL tetracycline, 100 μg/mL Bluo-gal, and 40 μg/mL IPTG) and confirmed by PCR. Bacmid DNA of wild-type recRPAP and mutants was used to transfect High 5 cells in the presence of Cellfect to prepare recombinant baculovirus, as described in the instruction manual of the bac-to-bac system of Life Technologies. The virus was amplified before use.

Purification of Wild-Type and Mutant Enzymes. Purification of wild-type recRPAP and the D146N, D146E, and D146A mutants was performed as described previously for recHPAP (*27*), with the exception that hydrophobic interaction chromatography was performed at pH 6.9 in MES buffer. Since wild-type recRPAP was found to be partly cleaved (10−15%) after purification, an additional FPLC step was used. RecRPAP was loaded onto a Pharmacia Mono S column preequilibrated with 50 mM MES, pH 6.5, 0.1 M KCl. The protein was eluted with 20 mL of a 0.1−0.5 M KCl gradient. Intact recRPAP was eluted at approximately 0.2−0.25 M KCl.

SDS−PAGE Analysis. SDS−PAGE was performed under reducing conditions essentially as described by Laemmli (*30*). Gels were either stained with Coomassie or blotted to immuno-PVDF membranes and probed with rabbit anti-recRPAP antiserum (diluted ×100) as the primary antibody and alkaline phosphatase-conjugated goat anti-rabbit IgG (diluted ×500) as the secondary antibody. Development was performed with NBT/BCIP. All steps were performed in accordance with the manufacturers' protocols.

Kinetics Measurements. (A) Enzyme Assay. Enzymatic activity was determined by monitoring the formation of the *p*-nitrophenolate anion at 410 nm ($\epsilon_{410nm} = 16.6$ mM^{-1} cm^{-1}) in a buffer containing 50 mM MES (pH 6.0), 300 mM KCl, 10 mM Na−K tartrate, 6.7 mM Na-ascorbate, 0.37 mM Fe-$(NH_4)_2(SO_4)_2$, and 50 mM *p*-NPP at 22 °C. At intervals after enzyme addition, 250 μL aliquots were removed and quenched with 1.0 mL of 0.5 M NaOH to convert all product to the phenolate form. The intact and cleaved FeZn forms of recRPAP were assayed in the absence of Na-ascorbate and $Fe(NH_4)_2(SO_4)_2$.

(B) pH Dependence. The pH dependence of k_{cat} was measured in 100 mM buffer (Na-acetate, MES, or HEPES), 300 mM KCl, 10 mM Na−K tartrate, 6.7 mM Na-ascorbate, 0.37 mM $Fe(NH_4)_2(SO_4)_2$, and *p*-NPP concentrations varied between 0.5 and 50 mM. For each determination of V_{max} and K_M, the hydrolysis rate was measured at six different *p*-NPP concentrations. After each assay, the pH of the reaction mixture was measured to ensure that it had not changed. Values of K_M and V_{max} were obtained by nonlinear regression using the program EnzymeKinetics (Trinity Software).

(C) Proteolytic Activation. Phosphatase activity was assayed in 96-well plates with *p*-NPP as substrate in 150 μL of incubation medium, pH 5.8, with the following final concentrations: 50 mM *p*-NPP, 1 mM ascorbic acid, 0.1 mM $Fe(NH_4)_2(SO_4)_2$, 0.1 M Na-acetate, 0.15 M KCl, 10 mM Na-tartrate, 0.1% (v/v) Triton X-100. The *p*-nitrophenol liberated after 1 h of incubation at 37 °C was converted to *p*-nitrophenolate by addition of 100 μL of 0.3 M NaOH, and the absorbance was measured at 405 nm ($\epsilon = 18.9$ mM^{-1} cm^{-1}) with a Spectramax 250 spectrophotometer (Molecular Devices, Sunnyvale, CA).

(D) Osteopontin. Enzyme assays with bovine milk osteopontin as substrate were performed essentially as described by Baykov et al. (*31*). Osteopontin (2−8 μM) was dissolved in the same buffer as used for the *p*-NPP assay, except the pH was 5.0 (total incubation volume 50 μL). The assay was stopped after 1 h at 37 °C by the addition of 50 μL of color reagent [0.12% malachite green in 3 M H_2SO_4, 7.5% ammonium molybdate, and 11% (v/v) Tween-20 (10:2.5:0.2 by volume)]. A phosphate curve (0−4 nmol) was always run in parallel. After color development for 30 min, the absorbance was read at 630 nm with a Spectramax 250 spectrophotometer.

Electron Paramagnetic Resonance (EPR) Spectroscopy. Samples contained 20% glycerol (v/v), and were frozen in liquid N_2. X-band EPR spectra (9.43 GHz) were obtained on a Bruker ECS106 EPR spectrometer equipped with an Oxford Instruments ESR900 helium-flow cryostat with an ITC4 temperature controller. The magnetic field was calibrated with an AEG Magnetic Field Meter, and the frequency was measured with an HP 5350B Microwave Frequency Counter.

Preparation of Zinc-Substituted RecRPAP. Half-apo-recRPAP was prepared as previously described for BSPAP (*32*). To 1 mL of 60 μM FeFe-recRPAP in 40 mM Na-acetate buffer, pH 5.0, 1.6 M KCl, and 20% glycerol were added 1 mM *o*-phenanthroline and 5 mM freshly prepared sodium dithionite. The release of Fe^{2+} was monitored by the absorbance of the $[Fe(phen)_3]^{2+}$ complex at 510 nm. After 3 min, the half-apo-enzyme was separated using a Sephadex

G-25 column, which was eluted with a Chelex-treated 40 mM Na-acetate buffer, pH 5.0, containing 1.6 M KCl and 20% glycerol. For reconstitution, the sample was incubated with a 20-fold excess of $ZnCl_2$ at room temperature for 5 h, followed by incubation overnight at 4 °C. Enzymatic assays and EPR measurements under reducing and oxidizing conditions confirmed that insignificant amounts of FeFe-recRPAP were present. The enzyme was used without further purification.

Proteolytic Digestion of RecRPAP. (A) Small-Scale Procedure. RecRPAP (wt, D146E, D146A, or D146N) was digested with cathepsin L at 37 °C for 2 h with the following final concentrations: PAP, 7 ng/μL; cathepsin L, 3 microunit/μL; 50 mM Na-acetate; 1 mM EDTA; and 2 mM DTT, pH 5.5. Cathepsin L was prereduced in 2 mM DTT for 7 min before it was added to the incubation solution. Trypsin (Sigma T-8003) digestion of recRPAP (wt, D146E, D146A, or D146N) was performed at room temperature for 45 min with the following final concentrations: PAP, 7 ng/μL; trypsin, 49.5 units/μL; 50 mM Tris-HCl, pH 7.5; 0.1 M NaCl; and 10 mM $CaCl_2$. Proteolytic digestions were stopped with proteinase inhibitor cocktail Complete (Roche) in accordance with the manufacturer's instructions.

(B) Large-Scale Procedure. One hundred twenty microliters of prereduced (7 mM DTT, 1 mM EDTA) cathepsin L (354 μg/mL) was added to a 1 mL solution (40 mM Na-acetate, pH 5.0) containing 2.1 mg/mL FeZn-recRPAP, 0.5 mM DDT, and 0.5 mM EDTA. After 2 h at room temperature, the sample was maintained at 4 °C overnight. Cathepsin L and other reagents were removed by repeated concentration/dilution using a Centricon (30 kDa cutoff).

RESULTS

Production of wild-type recRPAP and the three mutants by baculovirus-infected High 5 cells was followed by activity measurements. At 6 days post-infection, the activity was consistent with the presence of 6−12 mg of enzyme/L, and the culture was stopped. Purification of the four enzymes gave protein samples with R values (A_{280}/A_{515}) of 16−20, and a single band corresponding to the single-subunit form of PAP was observed for the mutants by SDS−PAGE under reducing conditions (not shown). Western blots (Figure S1) after kinetics and spectroscopic characterization revealed that small amounts of cleaved enzyme were present. The purified wild-type recRPAP contained 10−15% cleaved protein, which was separated from the intact form using an additional Mono S cation exchange chromatography step (*9*). UV−Vis spectroscopy of both wild-type enzyme and the mutants showed a maximal absorption at 515 nm (λ_{max}).

Reported pH optima for mammalian PAPs range from 4.7 to 6.3 (*9*, *27*, *33*). RecRPAP showed a nonGaussian pH optimum near 4.7, which shifted to 5.8 upon proteolytic cleavage (*9*). Similarly, early studies on BSPAP reported an optimal pH of 5.9 (*50*). These studies were, however, performed at a single nonsaturating substrate concentration, which can result in an apparent pH optimum that is significantly lower than the actual value. For example, measuring the pH optimum of Uf at high *p*-NPP concentrations gives a pH optimum that is 0.4 unit higher than reported (M. Pinkse, M. Merkx, and B. A. Averill, unpublished results), while more detailed studies gave a pH optimum of

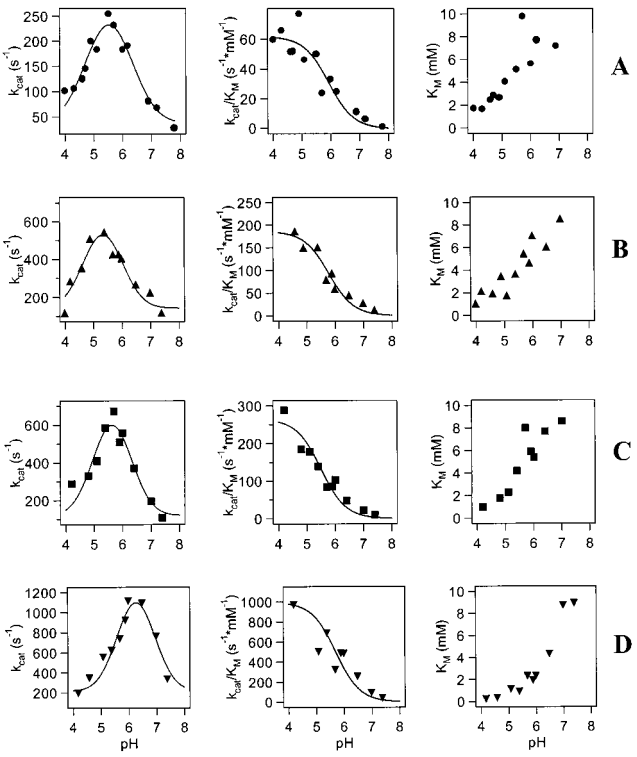

FIGURE 2: pH dependencies of k_{cat}, k_{cat}/K_M, and K_M for wild-type (A) and mutant Asp146Asn (B), Asp146Glu (C), and Asp146Ala (D) recRPAP with *p*-NPP as substrate at 22 °C. The lines represents fits of k_{cat} and k_{cat}/K_M to the rapid equilibrium diprotic model.

Table 1: Kinetics Parameters[a] of RecRPAP and D146 Mutants at 22 °C

	pH_{opt}	k_{cat} (s^{-1})	$pK_{es,1}$[b]	$pK_{es,2}$[b]	$pK_{e,2}$[c]
recRPAP	5.5	240	4.5	6.6	5.6
D146N	5.4	530	4.3	6.6	5.8
D146E	5.7	710	4.9	6.5	5.5
D146A	6.3	1310	5.5	7.1	5.7

[a] k_{cat} is defined as the number of substrate molecules hydrolyzed per enzyme molecule per second; $pK_{es,1}$ and $pK_{es,2}$ are for deprotonation/protonation events of a group of the enzyme−substrate complex; and pK_{e2} is for a deprotonation/protonation event of a group of the enzyme. K_S is defined as the dissociation constant of the ES complex. [b] Obtained from a fit of $k_{cat,obs}$ as a function of pH. [c] Obtained from a fit of $k_{cat,obs}/K_{M,obs}$ as a function of pH with $pK_{e1} < 2$.

6.5 for BSPAP (*29*). We therefore analyzed the pH dependence of k_{cat} of the wild-type and mutant recRPAPs by measuring V_{max} over the pH range 4−8 (Figure 2). The pH dependencies were analyzed according to a rapid equilibrium diprotic model (*34*), for which the following expressions were derived for the k_{cat} and k_{cat}/K_M (assuming that all equilibria are fast compared to k_{cat}).

$$k_{cat(observed)} = k_{cat}/(1 + [H^+]/K_{es,1} + K_{es,2}/[H^+]) \quad (1)$$

$$k_{cat(observed)}/K_{M(observed)} = k_{cat}/K_S(1 + [H^+]/K_{e1} + K_{e2}/[H^+]) \quad (2)$$

The pH optima and pK_a values obtained by fitting the data are given in Table 1. RecRPAP has a Gaussian pH optimum near pH 5.5, which is substantially higher than previously reported (pH 4.7) (*9*). The pH optima of the D146E (5.7) and D146A (6.3) mutants are higher, due to a shift of $pK_{es,1}$

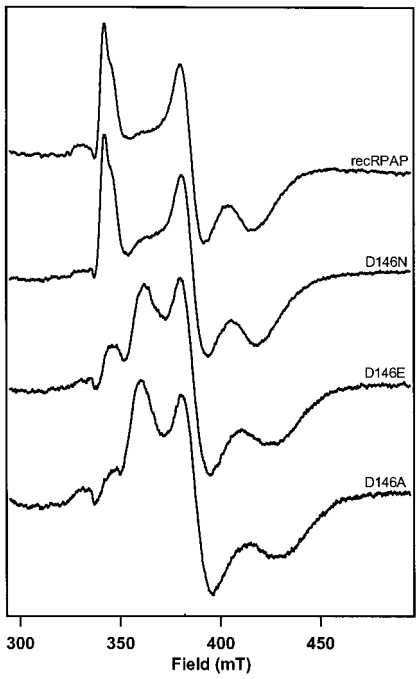

FIGURE 3: EPR spectra of single-polypeptide forms of wild-type and mutant recRPAP at pH 5.0. EPR conditions: microwave power, 2 mW; microwave frequency, 9.42 GHz; modulation, 12.7 G at 100 kHz; temperature, 4.5 K.

from 4.5 to 4.9 and 5.5, respectively. Except for the D146A mutant ($pK_{es,2} = 7.1$), the value of $pK_{es,2}$ is constant at around pH 6.6. k_{cat} for the mutants was up to 5 times greater than that of the wild-type enzyme (cf. 240 s^{-1} for recRPAP vs 1310 s^{-1} for the D146A mutant, at their respective pH optima). Although the pK_a values for the D146N mutant are not significantly different from those of the wild-type enzyme, k_{cat} is twice as large for the mutant. The D146E mutant showed a greater increase in k_{cat} (710 s^{-1}) compared to D146N (530 s^{-1}). Fitting of the k_{cat}/K_M values of all four forms using a single pK_a showed no significant change in $pK_{e,2}$. The K_M values of the mutants do not vary significantly.

Mammalian PAPs isolated as single polypeptide or proteolytically cleaved proteins exhibit characteristic EPR spectra. Typically, uncleaved proteins have a g_z value around 1.94, which is shifted to 1.86 in the cleaved proteins (*35*−*37*). As reported earlier (*29*), the EPR spectrum of intact wild-type recRPAP at pH 5.0 (Figure 3) has apparent *g*-values of 1.97 (with a shoulder at 1.94), 1.73, and 1.61. In the D146A mutant, where the interaction between Asp146 and Asn91 and/or His92 has been abolished, the g_z value was shifted to 1.86 and g_x to 1.58; some broadening of the EPR signal was also observed. The spectrum of the D146E mutant resembled that of a mixture of the intact and cleaved wild-type enzyme, with a small g_z feature at 1.97−1.94 together with a major feature at $g = 1.86$. Except for the presence of a small $g = 1.86$ signal, the EPR spectrum of the D146N mutant was essentially identical to that of the wild-type enzyme. A weak copper signal around $g = 2.05$ was observed in all spectra.

To investigate whether additional interactions are partially responsible for the low activity of the single-polypeptide form of the enzyme, cleavage of the mutant PAPs by proteases was performed. It has previously been demonstrated that the cysteine proteases papain and cathepsin B are more effective at activating RPAP than trypsin, and that cysteine proteases may be involved in proteolytic cleavage and activation of PAPs in vivo (*9*). Consequently, wild-type recRPAP and the D146N, D146E, and D146A mutants were treated with cathepsin L, which results in even higher activation than cathepsin B (J. Ljusberg and G. Andersson, unpublished results); the results are presented in Table 2. After cathepsin L digestion, the k_{cat} of all PAP forms investigated was about the same magnitude (2000−2400 s^{-1}), which is approximately 8-fold higher than that of wild-type recRPAP. Since the activities reported in Table 2 were measured at higher temperature, and at a single, nonoptimal pH, the values do not exactly parallel the k_{cat} values in Table 1. The proteolytically cleaved recRPAPs were analyzed by Western blots in order to confirm the expected cleavage pattern and the absence of monomeric PAP. Cathepsin L treatment converted all of the 36 kDa PAP forms examined into forms with subunit masses of 20 and 16 kDa, respectively (Figure S1).

Previous work showed that proteolytic cleavage of recRPAP with trypsin resulted in significantly less activation (*9*) than is observed for cleavage with cysteine proteases. Based on these results and MS experiments on recHPAP, we proposed that cleavage of a single peptide bond in the loop region results in a fragment that is held in place by noncovalent forces (*27*). To test this hypothesis, wild-type recRPAP and the D146A mutant were digested with trypsin. The activity of wild-type recRPAP increased 2.8-fold (268 versus 759 s^{-1}), while cleavage of the D146A mutant with trypsin gave no increase in activity (Table 2). Immunostained Western blots of the trypsin-digested preparations showed undetectable amounts of the single-polypeptide forms (data not shown).

Based on the crystal structure of RPAP, it was proposed that the low enzymatic activity of the uncleaved enzyme was due to steric interactions between the loop region and the substrate (*17*). The fact that the K_M value of a small (*p*-NPP) or a large (osteopontin, OPN) substrate molecule does not change significantly upon proteolysis of the enzyme indicates that steric effects are not responsible for the increase in activity observed upon proteolysis. To address this point directly, we examined the effect of proteolysis of wild-type recRPAP and the D146A mutant on their activity with a much bulkier substrate, the acidic phosphoprotein OPN, a putative in vivo substrate for PAP. The results (Table 3) show that cleavage by cathepsin increases the rate of hydrolysis of OPN 6.8-fold (11.5 versus 78.3 s^{-1}) for the wild-type protein and 4-fold (22.0 versus 89.0 s^{-1}) for the D146A mutant. Thus, comparable levels of activation are observed for both the wild-type enzyme and the D146A mutant with either *p*-NPP or OPN as substrate.

Based on the available crystal structures of mammalian PAPs, two specific interactions were suggested to be responsible for the differences between the intact and proteolytically cleaved enzymes: that between Asp146 and His92, which primarily affects the water/hydroxide bound to Fe^{3+}; and that between Asp146 and Asn91, which decreases the Lewis acidity of the divalent metal ion, thereby decreasing the electrophilicity of a substrate bound to that metal (*27*). Because the EPR spectrum of the $Fe^{3+}Fe^{2+}$ form of recRPAP is due to an antiferromagnetically coupled system with an $S = 1/2$ ground state, it is difficult to correlate changes in the EPR spectrum with changes in the environ-

Table 2: Activity[a] of Wild-Type (wt) RecRPAP and D146 Mutants after Proteolytic Digestion

	sp act.[b] (units mg^{-1})	k_{cat}[b] (s^{-1})	activation[c] (vs wt recRPAP)	K_M (mM)	k_{cat}/K_m ($\times 10^3$ M^{-1} s^{-1})	activation[d] (vs wt recRPAP)
wt recRPAP	459 (41)	268 (24)	1	3.4	79	1
+cat L	3617 (269)	2108 (157)	7.9	1.1	1916	24.2
+trypsin	1303 (44)	759 (26)	2.8	2.0	271	3.4
D146N	673 (97)	393 (57)	1.5	3.1	127	1.6
+cat L	3310 (327)	1929 (191)	7.2	1.1	1754	22.2
D146E	1551 (53)	904 (31)	3.4	3.2	283	3.6
+cat L	4205 (141)	2450 (82)	9.1	0.9	2722	34.5
D146A	2406 (85)	1402 (49)	5.2	2.1	668	8.5
+cat L	4225 (191)	2462 (111)	9.2	1.0	2462	31.2
+trypsin	1712 (91)	998 (53)	3.7	1.4	713	9.0

[a] Activity measurements were performed with *p*-NPP as substrate as described under Experimental Procedures under "Kinetics Measurements. (C) Proteolytic Activation". [b] Numbers in parentheses are standard deviation values. [c] Times activation of k_{cat}. [d] Times activation of k_{cat}/K_M.

Table 3: PAP Activity[a] with OPN as Substrate[b] at pH 5.8 and 37 °C

	sp act. (units mg^{-1})	k_{cat} (s^{-1})	activation[c] (vs wt recRPAP)	K_M (μM)	k_{cat}/K_m ($\times 10^3$ M^{-1} s^{-1})	activation[d] (vs wt recRPAP)
wt recRPAP	19.8	11.5	1	26.1	440.6	1
+cat L	134.3	78.3	6.8	22.3	3511	8.0
D146A	37.8	22.0	1.9	9.4	2340	5.3
+cat L	152.6	89.0	7.7	25.1	3546	8.0

[a] Activity measurements were performed with *p*-NPP as substrate as described under Experimental Procedures under "Kinetics Measurements. (C) Proteolytic Activation and (D) Osteopontin". [b] Mean values from two experiments. [c] Times activation of k_{cat}. [d] Times activation of k_{cat}/K_M.

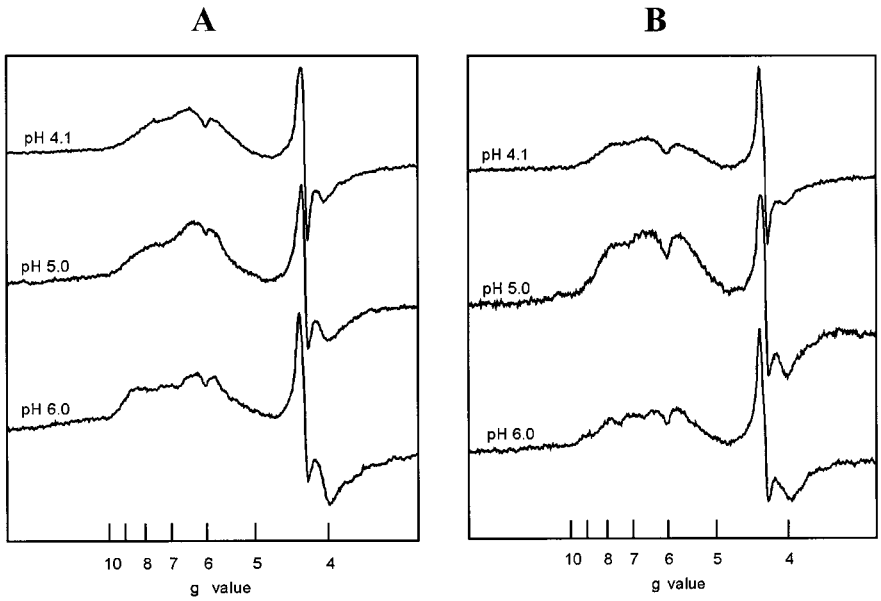

FIGURE 4: EPR spectra of single-polypeptide (A) and cathepsin L cleaved (B) forms of FeZn-recRPAP. EPR conditions: microwave power, 2 mW; microwave frequency, 9.42 GHz; modulation, 12.7 G at 100 kHz; temperature, 4.6 K.

ment of the individual components of the binuclear center. Substitution of high-spin ferrous ion ($S = 2$) by a diamagnetic metal such as Zn^{2+} results in an EPR spectrum due to the magnetically isolated high-spin ferric ion ($S = 5/2$) (*37*). The FeZn form of recRPAP was therefore prepared, and the effect of proteolytic cleavage was examined.

Intact FeZn-recRPAP had a λ_{max} of 525 nm, and its activity at pH 5.5 was considerably higher (800 s^{-1}) than that of the $Fe^{3+}Fe^{2+}$ protein (230 s^{-1}). The activity measured after incubation with H_2O_2 was the same as that measured in the presence of Fe^{2+}/ascorbate, indicating that significant amounts of the FeFe form were not present. Cleavage with cathepsin L produced fragments of mass 16 and 20 kDa, as shown by SDS−PAGE under reducing conditions. Kinetics measurements showed that proteolysis resulted in an increase in k_{cat} to 4200 s^{-1} at pH 6.2, with no change in K_M. As shown in Figure 4, the EPR spectra of intact and cleaved FeZn-recRPAP are essentially identical over the range pH 4.1−6.0. At pH 4.1, the spectra of both show peaks due to a mixture of high-spin Fe^{3+} species with rhombicities of $E/D = 0.02$ ($g = 6.5$ and 5.9 for the ground and middle Kramer's doublets, respectively), $E/D = 0.08$ ($g = 7.6$ and 5.8 for the ground and middle Kramer's doublets, respectively), and $E/D = 0.33$ ($g = 4.3$). At pH 6.0, both intact and cleaved recRPAP show additional features at $g = 7.0$ ($E/D = 0.05$) and $g = 8.8$ ($E/D = 0.17$). Thus, in contrast to $Fe^{3+}Fe^{2+}$-

recRPAP, proteolysis of FeZn-recRPAP produces no changes in EPR spectra at pH 5.0.

DISCUSSION

The mammalian purple acid phosphatases are single-polypeptide or two-subunit enzymes with molecular masses of 36 kDa, or 20 and 16 kDa, respectively. In addition, they differ in turnover number, pH optima, and EPR spectra at pH 5.0. The differences between these two species are due to proteolytic processing of an exposed loop near the active site (*9*, *26*, *27*), as can be seen by comparing the X-ray structures of rat bone PAP at 2.2 Å (*17*) and 2.7 Å (*18*) resolution. In the latter structure, the loop region [residues 146−161 according to the human sequence (*38*)] is absent, while in the former structure it is present and well-resolved. Mass spectrometry of recombinant human PAP revealed that a portion of this loop is removed by trypsin digestion (*27*). Western blot analysis of recRPAP cleaved with various proteases showed different fragmentation patterns (*9*), suggesting a correlation between enzymatic activation and the extent of cleavage and/or the identity of the cleavage sites (vide infra).

Based on the recently published X-ray structures of Uf and recRPAP, an interaction between this loop and the active site was proposed to be responsible for the kinetics and spectroscopic differences observed for various mammalian PAPs (*27*). The carboxylate side chain of Asp146 is well positioned to hydrogen bond to the amido group of Asn91, a ligand to the ferrous ion. Although the orientation is less favorable, the Asp146 carboxylate can also interact with the imidazole group of His92, which is located near the ferric ion and has been proposed to be involved in substrate binding. Analogous residues have been shown to be important in the protein phosphatases, whose catalytic sites are very similar to those of the purple phosphatases. In the protein phosphatases, Asn91 is a ligand to one of the metal ions, and it has been proposed to function in both catalysis and substrate coordination. Mutation of this residue to Asp, which is a better electron donor, results in a more acidic pH optimum and a decrease in activity. The Asn91Ala mutant shows a drastic decrease in catalytic activity, and the basic limb of the pH optimum was not observed in the pH versus activity plot (*39*). His92 of the protein phosphatases has been proposed to act as a general base catalysis that deprotonates an iron-coordinated solvent molecule (*25*, *28*), but isotope effect studies have not yet confirmed this proposal (*40*).

In the present study, we prepared mutants of recRPAP in which the loop residue Asp146 was mutated to the following: Asn, whose neutral but polar side chain should interact more weakly with both Asn91 and His92; Glu, with a longer side chain that in principle could still interact with His92; and Ala, whose small nonpolar side chain should completely abolish this interaction. The properties of the Asp146Ala mutant convincingly show that the interaction of this residue of the loop region with the binuclear iron site is responsible for the lower catalytic activity and pH optimum and the more rhombic EPR spectrum of the uncleaved wild-type enzyme. Moreover, these results show that activation does not depend on the presence of the loop, which excludes relief of steric hindrance as an explanation for the activation phenomenon (*17*). Consistent with this observation is the finding that the activation of both wild-type enzyme and Asp146Ala mutant upon proteolysis with cathepsin L does not depend on the size of the substrate. Although OPN is preferred to *p*-NPP as substrate (as shown by the higher k_{cat}/K_M values), the catalytic activity increases by approximately 4−8-fold for both *p*-NPP and OPN upon proteolysis. K_M for OPN increases upon proteolysis, in contrast to the observed reduction in K_M for *p*-NPP, further supporting the conclusion that activation is an electrostatic rather than a steric effect.

The properties of the Asp146Asn mutant do indeed show that reducing the strength of the electrostatic interaction of this side chain with the active site increases the catalytic activity and makes the EPR spectrum more axial, as shown by the shoulder at $g = 1.86$. It cannot be completely excluded that part of the higher activity and the shoulder in the EPR spectrum of the Asp146Asn mutant are due to the presence of small quantities of cleaved enzyme that were not detected with Coomassie staining (Figure S1). Based on calculations using the specific activity of highly purified recRPAP (*9*), the proportion of cleaved protein in the Asp146Asn should be approximately 15%, 8% for recRPAP, and 30−50% for the other mutants. Based on the SDS−PAGE results (Figure S1), this amount of cleaved protein could very well be present in the wild-type protein, but not in the mutant proteins. In the Asp146Glu mutant, it is clear that both the enzymatic turnover number and the pH optimum are higher than in the wild-type enzyme, which correlates nicely with the shift in $pK_{es,1}$ to higher pH. On the other hand, the EPR spectrum of this mutant is more affected than would be expected based on the 3-fold increase in activity. An explanation for this is provided by modeling of the three mutants in the Swiss-PdbViewer (http://www.expasy.ch/spdbv/mainpage.html by Glaxo Wellcome Experimental Research) and via Swiss-model (http://www.expasy.ch/swissmod/) (Figure S2). The modeled structure of the Asp146Glu mutant shows that the carboxylate side chain of the Glu points outward instead of inward toward the active site. Thus, the interaction with Asn91 is lost completely, but the distance between the carboxylate and His91 is unchanged (although the orientation for hydrogen bonding remains unfavorable). The structure of Uf (*16*) shows that water molecules are present in this region, which could form a hydrogen bonding network between the side chain and the iron site that affects the activity but not the Fe−Fe interaction, as shown by EPR spectra. Consequently, k_{cat} and the pH optimum might be expected to be affected less than the EPR spectrum, as is observed. These arguments imply that the interaction of Asp146 with Asn91 is more important than its interaction with His92, which is supported by the site-directed mutagenesis studies on PPs discussed above (*28*, *39*, *41*, *42*).

To examine the nature of the Asp146−active site interactions in more detail, we prepared the FeZn form of recRPAP. The EPR spectrum of this species should be quite sensitive to changes at the Fe^{3+} site and relatively insensitive to changes at the Fe^{2+} site (*33*). Since it is known that proteolysis alters the EPR spectrum of FeFe-recHPAP at pH 5.0 (*27*) and FeFe-recRPAP (unpublished results, E. G. Funhoff and B. A. Averill), the effect of proteolysis on the EPR spectrum of FeZn-recRPAP should allow us to distinguish between interactions with the trivalent and divalent metal sites. Proteolysis of FeZn-recRPAP with cathepsin L resulted in no significant changes in the EPR spectrum. This

result strongly suggests that the interaction between the loop region and the active site primarily involves the Fe^{2+} site, presumably via hydrogen bonding between the Asp146 carboxylate group and the Asn91 amido group.

Since there is a relationship between the site of cleavage and the specific activity of proteolyzed PAPs (*9*, *26*, *27*), the effect of proteolysis of recRPAP mutants by trypsin and cathepsin L was examined. The sequence of recRPAP indicates the presence of only a single trypsin cleavage site (after Arg157), presumably resulting in a "tail" that is held in place by noncovalent forces. Cathepsin L, however, displays a broad hydrolytic activity, especially toward substrates with hydrophobic residues. Consequently, it is capable of cleaving the exposed loop region at several sites and possibly excising the entire loop, as supported by SDS−PAGE analysis (*9*). If the only relevant interactions are those between Asp146 and His92 or Asn91, trypsin or cathepsin L digestion should not affect the activity of the Asp146Ala mutant. As shown in Table 2, however, treatment of the Asp146Ala mutant with cathepsin L results in an almost 2-fold increase in its enzymatic activity, while trypsin has no effect. Thus, interactions between other residues in the loop and the active site are also factors in the low catalytic activity observed for mammalian PAPs isolated as a single polypeptide.

Analysis of the interaction between the active site and the loop region of Uf and recRPAP with the program Chime (available at http://www.umass.edu/microbio/chime/find-ncb/index.html) showed that a hydrogen bonding network of water molecules is present in a cavity between the loop and the active site residues. This network results in additional interactions between the active site and the loop region, which could affect the enzymatic properties. In particular, hydrogen bonding of residues Gln151 and Gln152 water-mediated hydrogen bonding can occur either to His195, postulated to be involved in binding the substrate, or to one of the oxygen atoms of a bridging phosphate. The distances between the side chains of these residues and the water molecules vary between 2.5 and 3.1 Å, within the range of hydrogen bonding. The presence of a hydrogen-bonding network of water molecules can also explain the difference between the effects of cleavage by cathepsin L and trypsin. Since cathepsin L appears to remove the entire loop region, the effects of hydrogen bonding with Gln151 and Gln152 are lost upon treatment with cathepsin L but not with trypsin. The side chain of Ser145 is also capable of interacting with His221 and/or Asn91 (ligands to the Fe^{2+} ion), although less favorably. This residue is, however, present in the X-ray structure of cleaved recRPAP at 2.7 Å resolution (*18*), indicating that it is not part of the portion that is removed upon proteolysis.

In conclusion, we have shown that the interaction between residue Asp146 of the loop region and (an) active site residue(s) is the major factor in the observed differences between single-polypeptide and two-subunit forms of mammalian PAPs. Other interactions, such as water-mediated hydrogen bonding between residues in the loop region and the active site, are also present but are less important. Interactions between the loop and the active site primarily affect the divalent metal ion, and loss of these interactions upon proteolysis results in altered kinetics and spectroscopic properties. These results are consistent with the proposal that the nucleophilic hydroxide bridges the two metal ions (*43*−*45*), as has also been proposed for binuclear Ni and Zn enzymes (*46*−*48*). Our results do not support a mechanism in which the nucleophilic hydroxide ion is terminally bound to the trivalent (ferric) site (*33*, *49*−*53*), as has also been proposed for the PPs (*22*, *23*, *54*). Further studies on the identity of the nucleophile using different spectroscopic techniques are necessary to resolve this issue, and the differences between single-polypeptide and cleaved PAPs should be useful in this regard.

SUPPORTING INFORMATION AVAILABLE

Fragmentation pattern of recombinant RPAP after cathepsin L cleavage, and the modeled structures of the D146 mutants (2 pages). This material is available free of charge via the Internet at http://pubs.acs.org.

REFERENCES

1. Klabunde, T., and Krebs, B. (1997) *Struct. Bonding 89*, 177−198.
2. Vogel, A., Spener, F., and Krebs, B. (2001) *Handbook of metalloproteins* (in press).
3. Schenk, G., Ge, Y. B., Carrington, L. E., Wynne, C. J., Searle, I. R., Carroll, B. J., Hamilton, S., and deJersey, J. (1999) *Arch. Biochem. Biophys. 370*, 183−189.
4. Schenk, G., Korsinczky, M. L. J., Hume, D. A., Hamilton, S., and DeJersey, J. (2000) *Gene 255*, 419−424.
5. Oddie, G. W., Schenk, G., Angel, N. Z., Walsh, N., Guddat, L. W., De Jersey, J., Cassady, A. I., Hamilton, S. E., and Hume, D. A. (2000) *Bone 27*, 575−584.
6. Vallet, J. L., Christenson, R. K., and Mcguire, W. J. (1996) *Biol. Reprod. 55*, 1172−1178.
7. Buhi, W. C., Ducsay, C. A., Bazer, F. W., and Roberts, R. M. (1982) *J. Biol. Chem. 257*, 1712−1723.
8. Hayman, A. R., Warburton, M. J., Pringle, J. A. S., Coles, B., and Chambers, T. J. (1989) *Biochem. J. 261*, 601−609.
9. Ljusberg, J., EkRylander, B., and Andersson, G. (1999) *Biochem. J. 343*, 63−69.
10. Hayman, A. R., Jones, S. J., Boyde, A., Foster, D., Colledge, W. H., Carlton, M. B., Evans, M. J., and Cox, T. M. (1996) *Development 122*, 3151−3162.
11. Angel, N. Z., Walsh, N., Forwood, M. R., Ostrowski, M. C., Cassady, A. I., and Hume, D. A. (2000) *J. Bone Miner. Res. 15*, 103−110.
12. Hayman, A. R., Bune, A. J., Bradley, J. R., Rashbass, J., and Cox, T. M. (2000) *J. Histochem. Cytochem. 48*, 219−227.
13. Andersson, G., and EkRylander, B. (1995) *Acta Orthop. Scand. 66*, 189−194.
14. Ashkar, S., Weber, G. F., Panoutsakopoulou, V., Sanchirico, M. E., Jansson, M., Zawaideh, S., Rittling, S. R., Denhardt, D. T., Glimcher, M. J., and Cantor, H. (2000) *Science 287*, 860−864.
15. Sträter, N., Klabunde, T., Tucker, P., Witzel, H., and Krebs, B. (1995) *Science 268*, 1489−1492.
16. Guddat, L. W., McAlpine, A. S., Hume, D., Hamilton, S., de Jersey, J., and Martin, J. L. (1999) *Struct. Fold. Des. 7*, 757−767.
17. Lindqvist, Y., Johansson, E., Kaija, H., Vihko, P., and Schneider, G. (1999) *J. Mol. Biol. 291*, 135−147.
18. Uppenberg, J., Lindqvist, F., Svensson, C., EkRylander, B., and Andersson, G. (1999) *J. Mol. Biol. 290*, 201−211.
19. Durmus, A., Eicken, C., Spener, F., and Krebs, B. (1999) *Biochim. Biophys. Acta 1434*, 202−209.
20. Kissinger, C. R., Parge, H. E., Knighton, D. R., Lewis, C. T., Pelletier, L. A., Tempczyk, A., Kalish, V. J., Tucker, K. D., Showalter, R. E., Moomaw, E. W., Gastinel, L. N., Habuka, N., Chen, X., Maldonado, F., Barker, J. E., Bacquet, R., and Villafranca, J. E. (1995) *Nature 378*, 641−644.
21. Goldberg, J., Huang, H.-B., Kwon, Y.-G., Greengard, P., Nairn, A. C., and Kuriyan, J. (1995) *Nature 376*, 745−753.

22. Egloff, M. P., Cohen, P. T. W., Reinemer, P., and Barford, D. (1995) *J. Mol. Biol. 254*, 942−959.
23. Griffith, J. P., Kim, J. L., Kim, E. E., Sintchak, M. D., Thomson, J. A., Fitzgibbon, M. J., Fleming, M. A., Caron, P. R., Hsiao, K., and Navia, M. A. (1995) *Cell 82*, 507−522.
24. Vincent, J. B., and Averill, B. A. (1990) *FEBS Lett. 263*, 265−268.
25. Rusnak, F., and Mertz, P. (2000) *Physiol. Rev. 80*, 1483−1521.
26. Orlando, J. L., Zirino, T., Quirk, B. J., and Averill, B. A. (1993) *Biochemistry 32*, 8120−8129.
27. Funhoff, E. G., Klaassen, C. H. W., Samyn, B., Van Beeumen, J., and Averill, B. A. (2001) *ChemBioChem. 2*, 355−363.
28. Mertz, P., Yu, L., Sikkink, R., and Rusnak, F. (1997) *J. Biol. Chem. 272*, 21296−21302.
29. Ek-Rylander, B., Barkhem, T., Ljusberg, J., Ohman, L., Andersson, K. K., and Andersson, G. (1997) *Biochem. J. 321*, 305−311.
30. Laemmli, U. K. (1970) *Nature 227*, 680−685.
31. Baykov, A. A., Evtushenko, O. A., and Avaeva, S. M. (1988) *Anal. Biochem. 171*, 266−270.
32. Merkx, M., and Averill, B. A. (1998) *Biochemistry 37*, 11223−11231.
33. Merkx, M., Pinkse, M. W. H., and Averill, B. A. (1999) *Biochemistry 38*, 9914−9925.
34. Segel, I. H. (1993) *Enzyme Kinetics: Behaviour and analysis of rapid equilibrium and steady-state enzyme systems*, John Wiley & Sons, New York.
35. Sinn, E., O'Connor, C. J., de Jersey, J., and Zerner, B. (1983) *Inorg. Chim. Acta 78*, L13-L15.
36. Debrunner, P. G., Hendrich, M. P., de Jersey, J., Keough, D. T., Sage, J. T., and Zerner, B. (1983) *Biochim. Biophys. Acta 745*, 103−106.
37. Davis, J. C., and Averill, B. A. (1982) *Proc. Natl. Acad. Sci. U.S.A. 79*, 4623−4627.
38. Lord, D. K., Cross, N. C. P., Bevilacqua, M. A., Rider, S. H., Gorman, P. A., Groves, A. V., Moss, D. W., Sheer, D., and Cox, T. M. (1990) *Eur. J. Biochem. 189*, 287−293.
39. Zhang, J., Zhang, Z. J., Brew, K., and Lee, E. Y. C. (1996) *Biochemistry 35*, 6276−6282.
40. Hoff, R. H., Mertz, P., Rusnak, F., and Hengge, A. C. (1999) *J. Am. Chem. Soc. 121*, 6382−6390.
41. Zhuo, S., Clemens, J. C., Stones, R. L., and Dixon, J. E. (1994) *J. Biol. Chem. 269*, 26234−26238.
42. Huang, H. B., Horiuchi, A., Goldberg, J., Greengard, P., and Nairn, A. C. (1997) *Proc. Natl. Acad. Sci. U.S.A. 94*, 3530−3535.
43. Wang, X. D., Ho, R. Y. N., Whiting, A. K., and Que, L. (1999) *J. Am. Chem. Soc. 121*, 9235−9236.
44. Yang, Y. S., McCormick, J. M., and Solomon, E. I. (1997) *J. Am. Chem. Soc. 119*, 11832−11842.
45. Wang, X., Randall, C. R., True, A. E., and Que, L., Jr. (1996) *Biochemistry 35*, 13946−13954.
46. Yamaguchi, K., Cosper, N. J., Stalhandske, C., Scott, R. A., Pearson, M. A., Karplus, P. A., and Hausinger, R. P. (1999) *J. Biol. Inorg. Chem. 4*, 468−477.
47. Benini, S., Rypniewski, W. R., Wilson, K. S., Miletti, S., Ciurli, S., and Mangani, S. (2000) *J. Biol. Inorg. Chem. 5*, 110−118.
48. Carfi, A., Duee, E., PaulSoto, R., Galleni, M., Frere, J. M., and Dideberg, O. (1998) *Acta Crystallogr., Sect. D: Biol. Crystallogr. 54*, 47−57.
49. Dietrich, M., Münstermann, D., Suerbaum, H., and Witzel, H. (1991) *Eur. J. Biochem. 199*, 105−113.
50. Aquino, M. A. S., Lim, J.-S., and Sykes, A. G. (1994) *J. Chem. Soc., Dalton Trans.*, 429−436.
51. Pinkse, M. W. H., Merkx, M., and Averill, B. A. (1999) *Biochemistry 38*, 9926−9936.
52. Merkx, M., and Averill, B. A. (1999) *J. Am. Chem. Soc. 121*, 6683−6689.
53. Klabunde, T., Sträter, N., Fröhlich, R., Witzel, H., and Krebs, B. (1996) *J. Mol. Biol. 259*, 737−748.
54. Voegtli, W. C., White, D. J., Reiter, N. J., Rusnak, F., and Rosenzweig, A. C. (2000) *Biochemistry 39*, 15365−15374.

BI010766R